JOURNAL OF MATERIALS SCIENCE 23 (1988) 3305–3313

Fatigue behaviour of sintered SiC; temperature dependence and effect of doping with aluminium

SUSUMU HORIBE, MASAE SUMITA
National Research Institute for Metals, Sengen, Sakura-mura, Ibaraki 305, Japan

Cyclic and static fatigue behaviours were investigated using sintered β-SiC materials with indentation-induced precracks, focusing especially on the temperature dependence and the effect of doping with aluminium. No effects of cyclic loading were observed in the crack growth of materials both with and without aluminium, tested for the whole temperature range of room temperature to 1500° C, suggesting that cyclic fatigue might be insignificant in SiC. However, there is static fatigue damage in the material, the causes of which seem to be different depending upon the temperature and the aluminium doping. The static fatigue observed at room temperature is environmentally assisted cracking, whereas the fatigue at high temperature (1500° C) seems to be controlled by the creep properties. In the high-temperature behaviour, doping SiC with aluminium makes its strength decrease for the case where the material is loaded to failure in a short time, but makes the resistance to cracking rather increase for the case where the sample is statically loaded at lower stresses for a relatively long time.

1. Introduction

Studies of the fatigue phenomena in ceramic materials are very important not only for engineering practice but also to understand more deeply the fundamental mechanism of fracture in non-metallic bonded materials. However, these have not been sufficiently studied and there are a lot of uncertain matters awaiting solution. It seems to be one of the most essential topics in many kinds of ceramic material to determine whether cyclic loading really results in the accumulation of damage which is not simply predictable from the static fatigue data.

SiC and Si_3N_4 are promising materials as a focus of attention for high-temperature use. For Si_3N_4, there have been some investigations on cyclic fatigue [1–5], and Kawakubo and Komeya [5] have reported that there might exist a cyclic loading effect. The present author [6] also has recently found that some fatigue crack propagation is not affected by static loading but only caused by load cycling, and pointed out that this might be interpreted by fracture mechanics as is the case with metallic materials. On the other hand, in SiC also there are a couple of reports suggesting the fatigue damage of materials under cyclic loading conditions [3, 7]. It is not clear, however, if such damage is completely cycle-dependent, and rather there is a possibility that it might be time-dependent. In other words, so far there have been no reports on the distinct effect of cyclic loading on the fatigue damage of SiC.

In the present study, we have investigated the cyclic and static fatigue phenomena of two kinds of sintered β-SiC material, trying to separate and clarify both phenomena for the wide temperature range of room temperature (RT) to 1500° C.

2. Experimental procedures

2.1. Specimens

Two kinds of material (S-1 and S-2) were prepared by using powders P-1 and P-2, the characteristics of which are listed in Table I. The main difference between them is in the aluminium content; P-2 contains 0.39 wt % Al. Both powders were sintered with the aid of boron and carbon to produce S-1 and S-2 materials with the densities shown in Table II. Such preparation of specimens was carried out by Ibiden Co. Ltd.

In most specimens the precracks were introduced by Vickers indentation (and Knoop indentation for a couple of other specimens) prior to fatigue testing. An indentation load of 49 N was mainly used for the specimens for the RT tests and 9.8 N indentation loading was adopted for high-temperature testing. A higher load seems to be desirable for fatigue testing because it diminishes the experimental scatter. In the present experiments at high temperatures, however, when the chamber is being evacuated prior to the introduction of inert gas the specimen is inevitably loaded, because in order to get a good fitting of the specimens with the four-point fulcra they need to be in contact and to be adjusted manually in the ambient air. Accordingly, if a specimen should have a large initial crack, it may fail during evacuation. This is why

TABLE I Properties of SiC powders (chemical composition, specific surface area S and average grain diameter D)

Powder	Content (wt %)				S ($m^2 g^{-1}$)	D (μm)
	SiO_2	C	Al	Fe		
P-1	0.34	0.36	0.03	0.04	20.0	0.26
P-2	0.53	0.53	0.39	0.07	21.9	0.29

0022–2461/88 $03.00 + .12

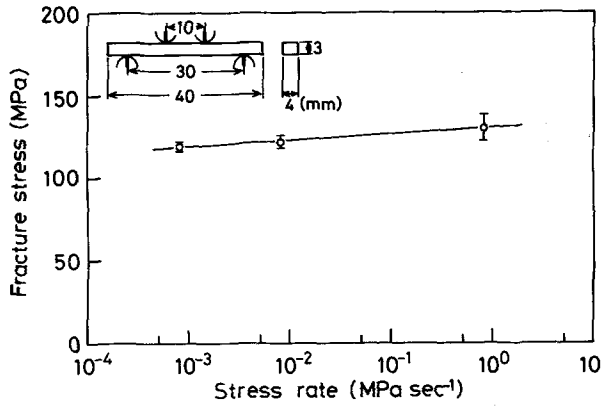

Figure 1 Dynamic fatigue data for S-1 showing the relationship between fracture stress and stress rate in air at room temperature. Each point is the average value for three specimens tested. Vickers indentation, 49 N.

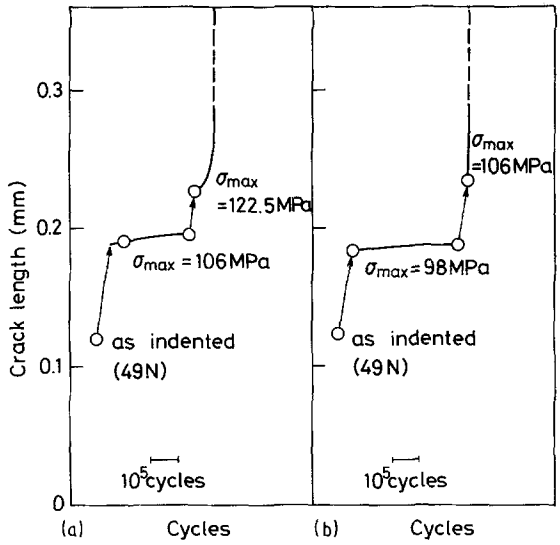

Figure 2 Crack propagtion observed during cyclic loading in air at room temperature: (a) S-1, (b) S-2.

for inert-gas testing at high temperatures the lower indentation load (9.8 N) was adopted.

2.2. Fatigue testing

Dynamic, static and cyclic fatigue tests were conducted on the above two types of material by the four-point bending method, using a hydraulic fatigue-testing machine. The size of the specimen for fatigue testing is shown in Fig. 1. Test temperatures were RT, 770 and 1500° C. Testing at RT was carried out in air and the other testing at high temperatures was in pure argon gas. In cyclic fatigue a sine-wave loading was used at a stress ratio $R = 0.2$ and a frequency of 1 to 3 Hz for the non-creep range (RT and 770° C), whereas a trapezoidal wave (time of holding at the maximum stress = 5 sec) was used under creep conditions (1500° C).

3. Results and discussion

3.1. Fatigue properties at room temperatures

Fig. 1 shows the dynamic fatigue property of S-1 material, in which precracks were introduced in advance by Vickers indentation, in the stress rate range of 10^{-3} to 10^{0} MPa sec^{-1} in ambient air. Although the number of specimens is limited and there is some scatter at the highest stress rate, a very slight but significant loading-rate dependency was observed, which suggests that there exists an environmentally assisted cracking in this material. Evans and Lange [8] have shown no dependence of stress rate on the flexural strength of hot-pressed SiC at 25° C, which differs from the present data. This may be because the range of stress rate they used is higher than ours.

Figs 2a and b exhibit the cyclic fatigue properties of the materials S-1 and S-2, respectively. Crack advancement was certainly observed during cycling loading. However, under the static loading condition shown in Fig. 3* also there is a tendency for crack propagation. These results mean that there obviously

TABLE II Additives and density of sintered SiC

Specimen	Powder	Additives	Density (g cm^{-3})
S-1	P-1	1 wt % B–2 wt % C	3.05
S-2	P-2	0.1 wt % B–2 wt % C	3.12

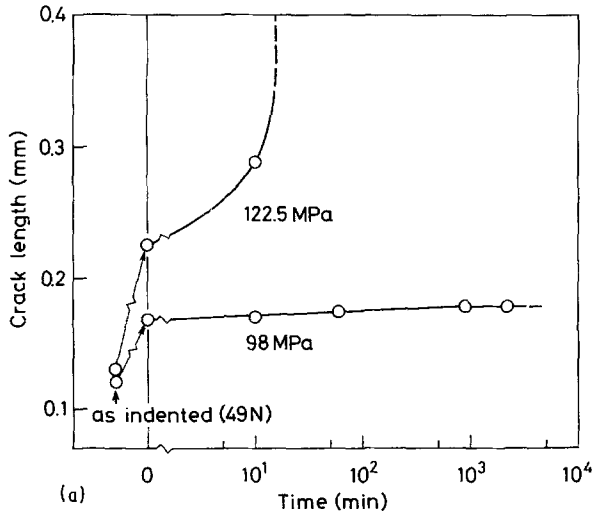

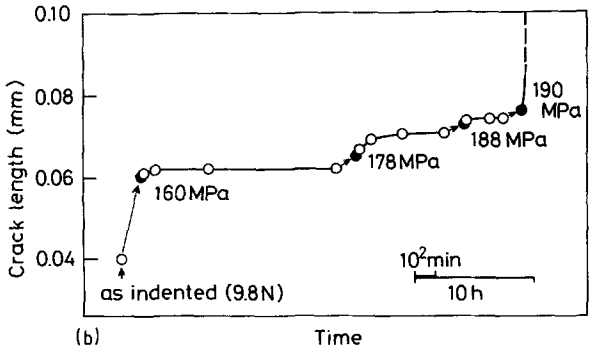

Figure 3 Crack propagation in S-1 during static loading in air at room temperature: indentation of (a) 49 N, (b) 9.8 N loading.

*Closed symbols indicate the first measured point for each stress level in Fig. 3 and later figures.

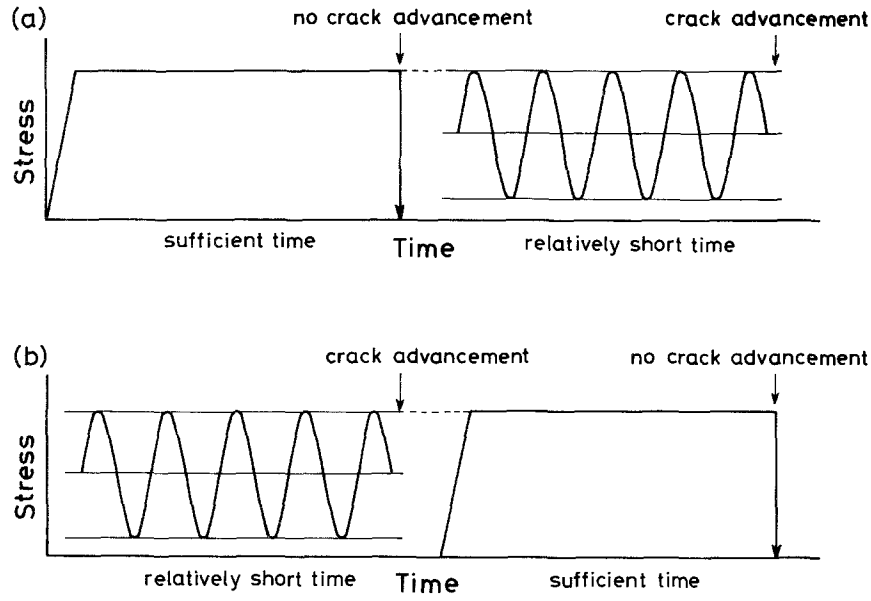

Figure 4 Simple and reliable method to check the damage caused by cyclic loading.

exists a time-dependent fracture which seems to be caused by the environment, but it is doubtful whether the repetition of the loading itself makes the crack advance or not; there is a possibility that in the cyclic loading process a factor of the static loading (the time-dependent component) alone makes the crack propagate. It is noted in Figs 2 and 3 that since the specimens were loaded slowly at the stress rate of 0.82 MPa sec^{-1} to each stress level to avoid stress-overshooting, the crack might inevitably propagate for a certain distance during the load increase.

In order to check whether or not there exists a cyclic effect in this material, the most simple and reliable method is proposed in Fig. 4. Figs 4a and b are essentially the same. For evidence of a cyclic effect which is not influenced by the environment, both of the following conditions must be observed; (i) no crack advancement under static loading for sufficient time, and (ii) crack advancement during cyclic loading with the same stress as the maximum one. Since it is usual that the fatigue data differ from one specimen to another, this method is recommended to be carried out using a single specimen. Fig. 5 shows the results obtained by the method of Fig. 4a. For the S-1 material (Fig. 5a) during static fatigue at an applied stress below 118 MPa, the crack propagates rapidly at an early time and is soon arrested. In the subsequent cycling at each step, significant crack advancement is not observed. It has been found, therefore, that there is no effect of load cycling on the crack advancement in this material at room temperature. The static fatigue crack at an applied stress of 122.5 MPa propagated very rapidly without arresting and final fracture occurred. In the material S-2 also a similar

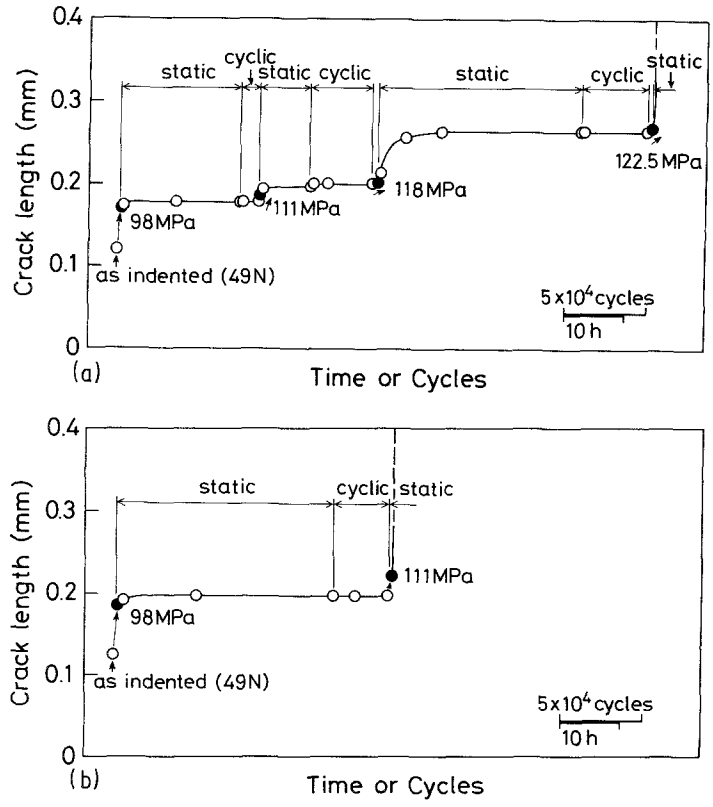

Figure 5 Fatigue crack propagation during cyclic or static loading in air at room temperature obtained in the manner of Fig. 4a: (a) S-1, (b) S-2.

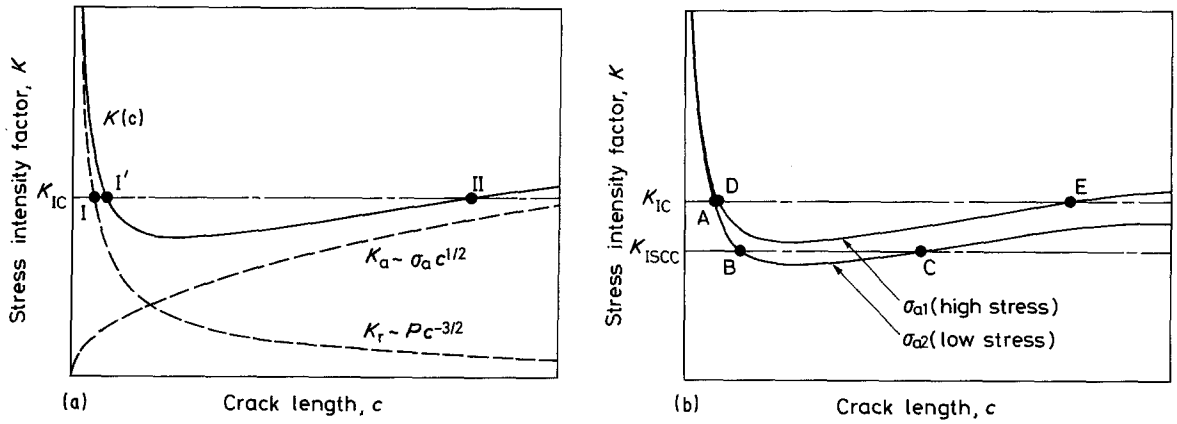

Figure 6 Configuration of stress intensity factor K as a function of crack length c: (a) indentation load and applied stress are fixed (from [9]), (b) the K configurations for two levels of applied stress are schematically shown.

tendency has been observed, as shown in Fig. 5b, although it tends to fail at a lower stress level.

Crack arrest observed at the lower applied stresses seems to be peculiar to specimens having an indented crack. The stress intensity factor K which is a function of crack length c is qualitatively illustrated in Fig. 6a. Crack growth under equilibrium and non-equilibrium conditions is explained in detail by Marshall and Lawn [9]. The K value is the summation of a term K_r due to the residual stress and a term K_a caused by the applied stress. In a fixed indentation condition, the crack behaviour is determined by the applied stress and the environment. On the application of stress the crack grows spontaneously from Point I to Point I'.

Fig. 6b shows two levels of K configuration in relation to the fracture toughness value K_{IC} and the threshold stress intensity factor affected by the environment K_{ISCC} values. In the case where the applied stress is σ_{a2}, the point I' is indicated by Point A in this figure. Subsequently, this crack propagates time-dependently from Point A to Point B. Point B corresponds to K_{ISCC}. In this region (from A to B) the further the crack propagates the more the K value decreases, which causes early rapid crack growth and the subsequent low-rate crack growth and arresting, as observed in Figs 3 and 5. No further crack advancement beyond Point B is expected in such a static fatigue condition. If the crack should be advanced from Point B to Point C by any means (e.g. by cyclic loading), the crack could again propagate from C under the preceding static fatigue condition. The present results in Fig. 5 show, however, that load cycling is not effective for crack advancement in this material. In the case of σ_{a1}, the crack propagates subcritically from Point D to Point E depending on the environment, and the material fails abruptly at Point E.

3.2. Fatigue properties at high temperatures

Fig. 7 exhibits the crack propagation behaviour of materials statically or cylically loaded at 770° C in argon gas. In contrast with the behaviour at room temperature in air, subcritical crack growth was not observed under static nor cyclic loading, although in S-2 material a slight crack growth was seen in static loading at the first stress level. This indicates that the fracture of SiC under these conditions hardly depends on the time or the number of cycles, but only on the tensile stress level (which is of course affected by residual stresses).

Fig. 8 shows the relationship between stresses and strains in the case where the precracked materials were loaded at the rate of 0.82 MPa sec^{-1} at 1500° C. S-1, which does not contain aluminium, is high in strength

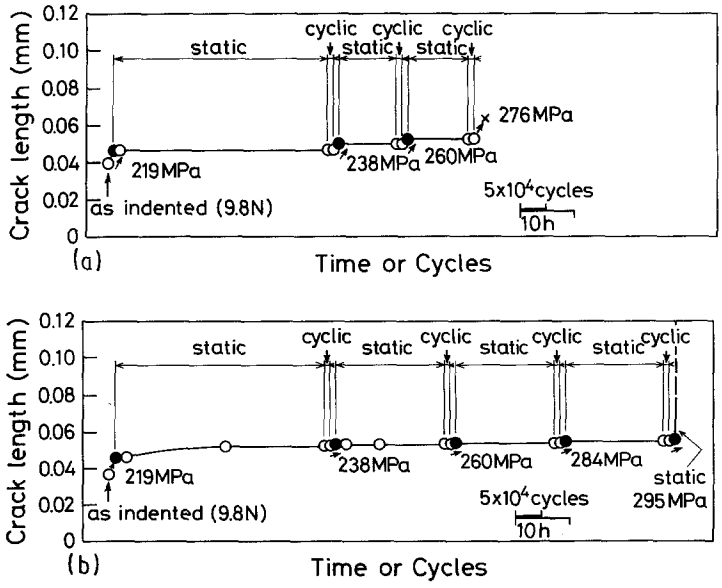

Figure 7 Fatigue crack propagation during cyclic or static loading in argon gas at 770° C obtained in the manner of Fig. 4a: (a) S-1, (b) S-2.

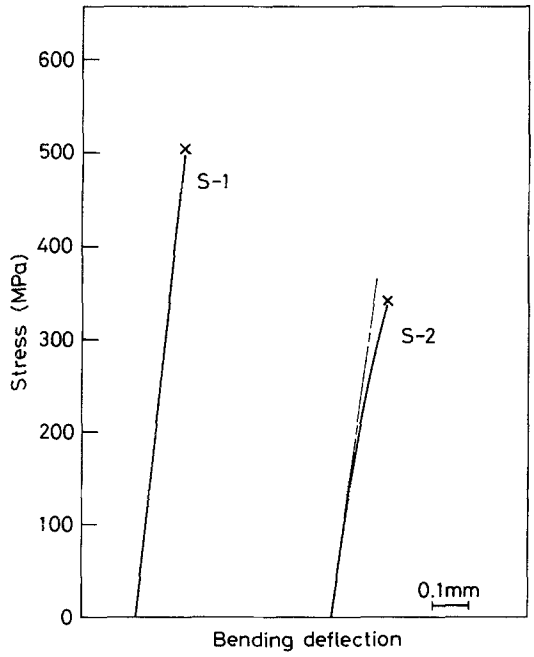

Figure 8 Relationship between stress and bending deflection in argon gas at 1500° C (stress rate 8.2 × 10^{-1} MPa sec^{-1}, indentation load 9.8 N).

but shows negligibly small plastic deformation until the final fracture. On the other hand, S-2 which contains aluminium is low in strength but has a high ductility. Fig. 9 represents the relationship between the strain (bending deflection) and the number of cycles (and time) during cycling. The specimens were statically loaded at the maximum values of the subsequent cyclic stresses for the first 70 min (static fatigue) and then cyclically loaded. From these results it is clear that S-2 shows a larger deformation in comparison with S-1 in both creep conditions of static fatigue and cyclic fatigue. Both materials are cyclically loaded by the stress normalized by the fractured stress ($0.89\sigma_f$) but the cyclic fatigue lives for both materials seem to be different; S-1 fractured at 7.7 × 10^3 cycles (ca. 16 h), whereas S-2 did not. Macrographs of smooth specimens cycled at σ_{max} = 300 MPa and R = 0.28 for the same number of cycles, shown in

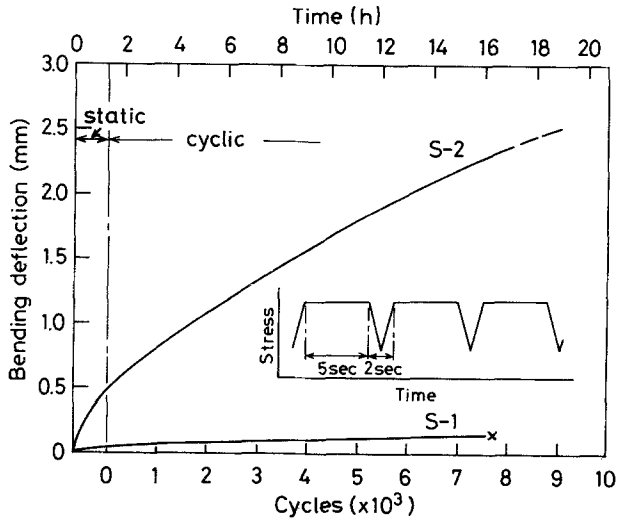

Figure 9 Variation of bending deflection during cyclic loading in argon gas at 1500° C (σ_{max} = $0.89\sigma_f$, R = 0.28, indentation 9.8 N).

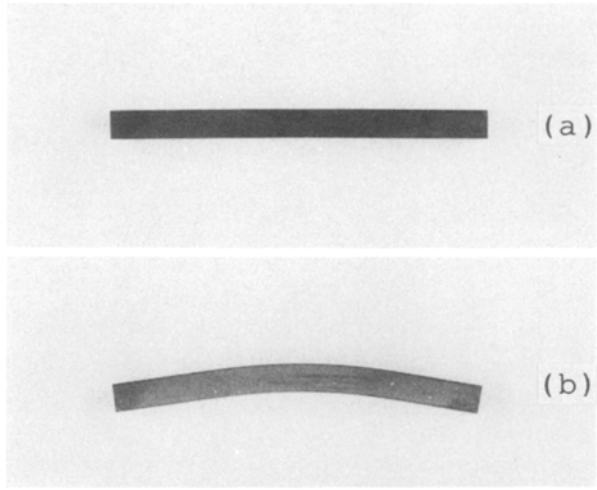

Figure 10 Smooth specimens cyclically loaded at 300 MPa in argon gas at 1500° C (R = 0.28, N = 7.7 × 10^3 cycles): (a) S-1, (b) S-2.

Fig. 10, indicates that the material containing aluminium tends to undergo considerable plastic deformation, irrespective of the existence of a crack. Therefore, it is concluded that aluminium doping decreases the fracture strength of SiC under conditions where the load is applied to the specimen for a short time at high temperature, whereas aluminium is desirable for strength and ductility under relatively low stress loading for a long time.

Fig. 11 exhibits the surface flaw morphologies of material in which the microcrack was introduced by a Knoop indentor (9.8 N), cyclically loaded at high temperature. The crack tends to propagate slowly in S-2 material, the crack tip of which becomes blunted. In contrast, such crack behaviour was not observed in S-1 material. It should be noted here again that S-1 fails at earlier times than S-2 (Fig. 9) in spite of the trend of the slow crack growth in S-2. In order to understand the details of these interesting results, further study is needed, but without doubt aluminium doping is relevant to high ductility or to a crack-tip blunting effect at high temperature. Therefore, we can expect the development of superior SiC materials by controlling the aluminium content.

To observe the fractured surface at high temperature, the specimens were broken at room temperature. Scanning electron microscopy (SEM) pictures of S-2 and S-1 materials are shown in Figs 12 and 13, respectively. Region A in Fig. 12 is the fractured surface produced at high temperature. SEM at high magnification (Fig. 12b) shows intergranular cracking, and it is assumed that such cracking is preceded by grain boundary sliding and the cavitation process. On the other hand, in S-1 material intergranular fracture was not observed, and even the borders of the fractured areas at high temperature and at room temperature were not clear (Fig. 13).

As mentioned above, significant differences of deformation and crack behaviours between the two types of material under cyclic conditions at 1500° C were interestingly observed. However, it should be noted that these are not peculiar to cyclic loading, but might be seen in static loading in the same manner. In support of this result, Fig. 14 shows the deflection rate

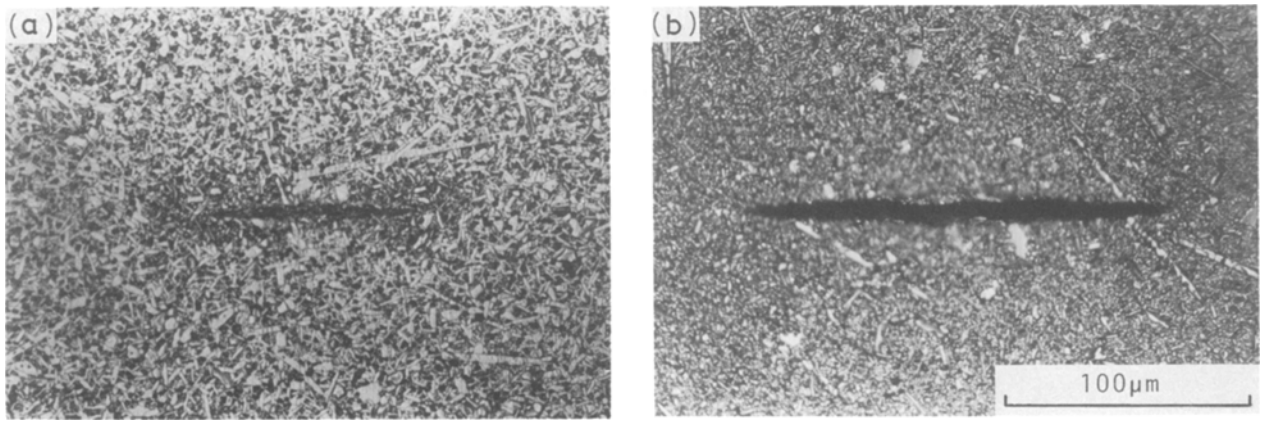

Figure 11 Example of crack morphology after cyclic fatigue in argon gas at 1500° C (9.8 N Knoop indentation, σ_{max} = 300 MPa, R = 0.28): (a) S-1, (b) S-2.

measured under conditions of static and cyclic loadings using a single smooth specimen. The deflection rate in the static condition is sited between the two kinds of value for cyclic conditions which are calculated from the same data; in the upper curve the holding time at maximum stress is adopted for the calculation of the creep rate, whereas in the lower curve the total time for cycling is used. It is concluded, therefore, that the effect of cyclic loading on creep behaviour is also insignificant.

3.3. Effect of the environment on static fatigue at room temperature

The experiments at room temperature were conducted in air, which showed that the crack is advanced by static loading (Fig. 3). In order to clarify the extent of this effect and to obtain coherency between the data at RT (in air) and at high temperatures (in argon gas), static fatigue tests were carried out at RT in air and in argon gas using specimens indented at 9.8 N load (Fig. 15). From this figure it is clear that the crack growth under static loading conditions is affected by the environment and is much limited in inert gas. Accordingly, it seems natural that in the test at 770° C the static fatigue crack growth was negligible.

3.4. Temperature dependence of fracture stress

Fig. 16 shows the temperature dependence of fracture stress of indented specimens at 9.8 N load. With increase of temperature the fracture stresses increase. It seems that this result, obtained by testing in argon gas, differs from the data on hot-pressed SiC tested in air and in a vacuum by Petrovic and Jacobson [10], although the precise reason for this is not clear. Furthermore, it is of interest that the extent of the increment is larger in S-1 than in S-2. It has been assumed that the higher resistance to fracture at enhanced temperatures might be attributed to the relaxation of residual stresses [11] and to the healing of

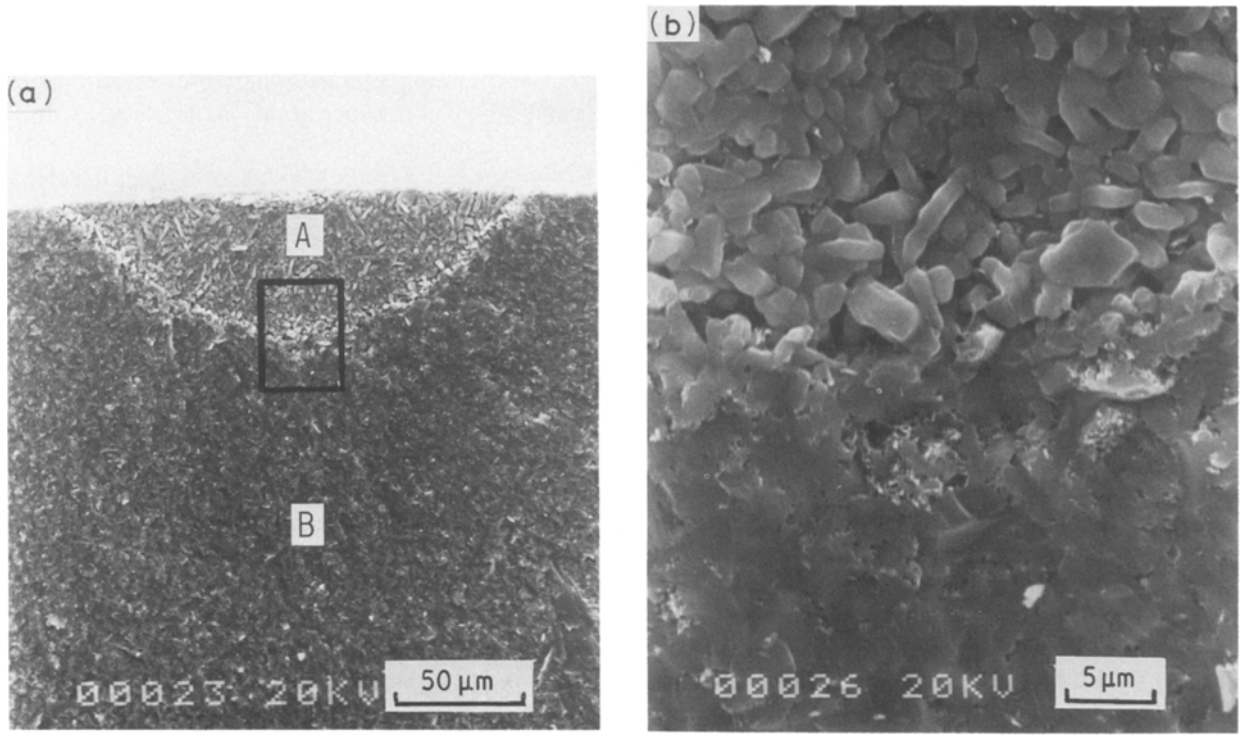

Figure 12 Fracture surface of the S-2 specimen shown in Fig. 11b which was broken at room temperature: (a) low magnification, (b) high magnification.

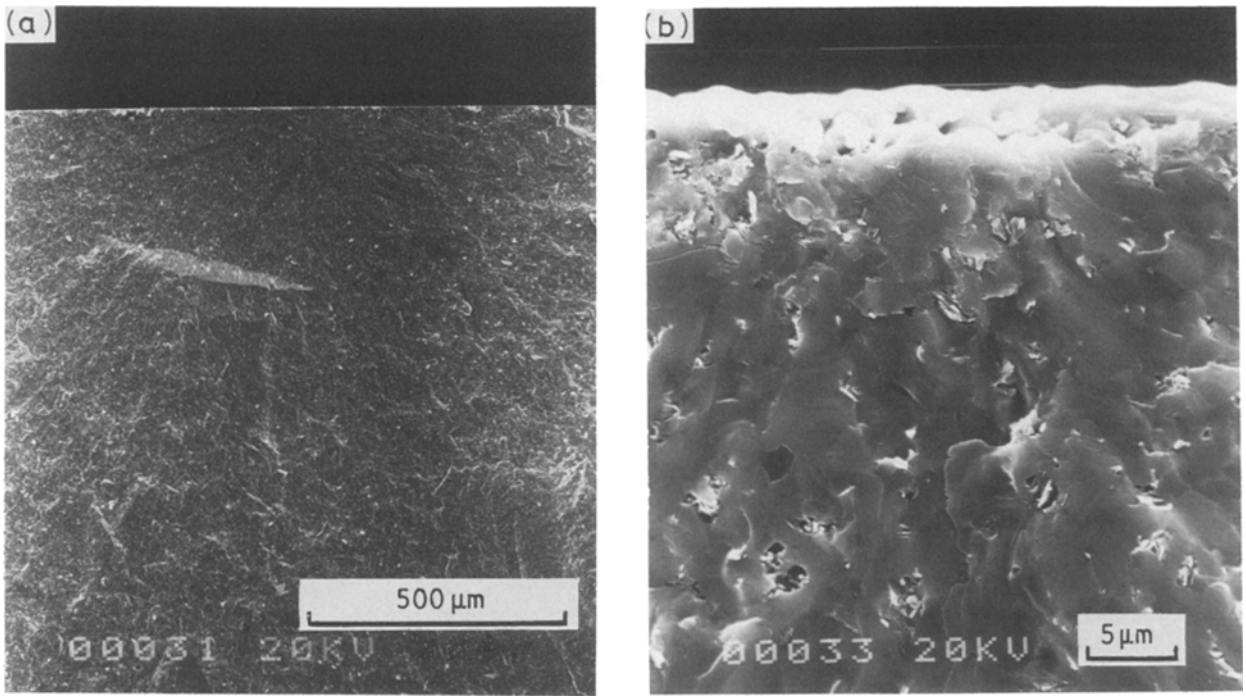

Figure 13 Fracture surface of the S-1 specimen shown in Fig. 11a which was broken at room temperature: (a) low magnification, (b) high magnification.

flaws [12, 13]. The flaw healing which occurs at 1500° C under the present experimental conditions might be caused by crack tip blunting during loading and by the decrease of crack size due to re-sintering (or oxidation.)

It is obvious from the crack tip morphology (Fig. 11) that the crack tip blunting at 1500° C is more remarkable in S-2 compared to S-1. Interestingly, in spite of that, S-1 has a higher resistance for fracture. Accordingly, it is assumed that this high resistance to cracking in S-1 might be mainly due to the decrease of the crack size caused by re-sintering or oxidation. There is evidence for this assumption. All the specimens with 9.8 N indentation-precracks tested at various temperatures were broken into two pieces by propagation of the initial crack except for the S-1 specimen tested at 1500° C (Fig. 17a). It was observed in this S-1 at 1500° C that the specimen was broken into several pieces, as shown in Fig. 17b, although the initial flaw is always one of the fatal cracks. This indicates that the initial flaw in S-1 material put in such a high-temperature environment is no longer the dominant crack which makes the material separate into two parts. However, in order to understand the details of the micromechanism of this fracture and the

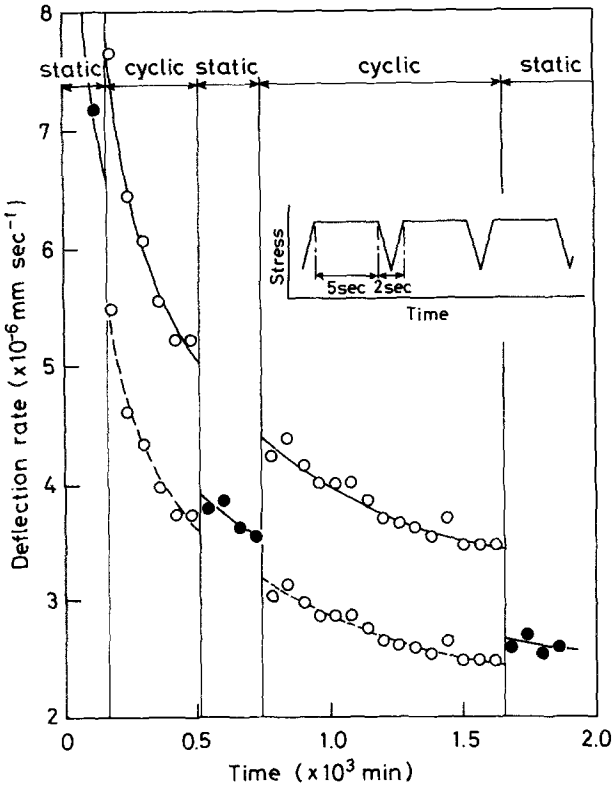

Figure 14 Variation of creep rate (deflection rate) in smooth S-2 specimen fatigued in cyclic and static loadings alternately. The explanation for the two kinds of curve in cyclic fatigue is given in the text.

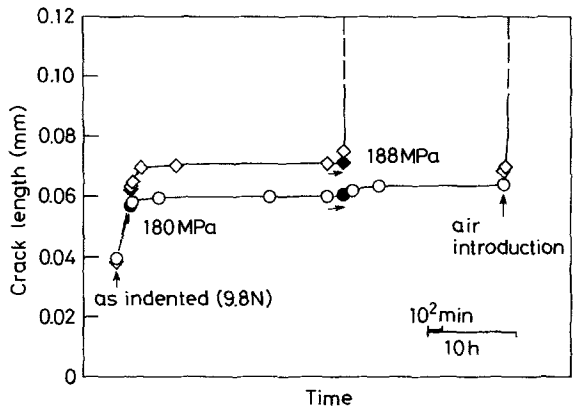

Figure 15 Effect of the environment on the static fatigue crack growth of S-1 at room temperature in (◇) air and (○) argon gas. Note that the crack arrested in argon restarts to propagate on the introduction of air.

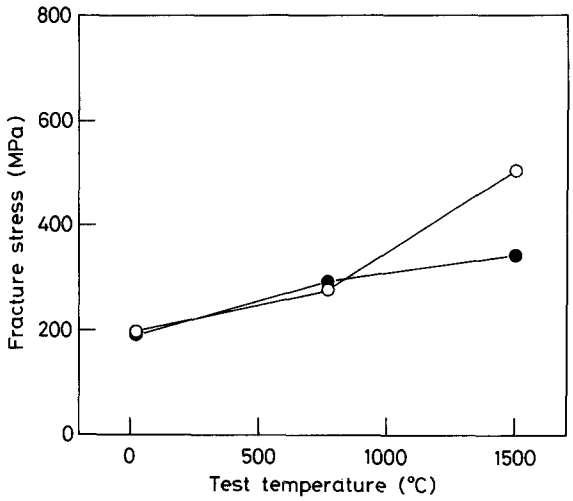

Figure 16 Temperature dependence of the fracture stress of SiC materials (stress rate 8.2×10^{-1} MPa sec^{-1}, indentation load 9.8 N): (○) S-1, (●) S-2.

differences between the two materials further studies are needed.

3.5. Effect of aluminium doping on the fatigue behaviour at elevated temperature

The effects of aluminium on the deformation and fracture of SiC have been studied by some researchers [12–15]. Moussa *et al.* [14] have tested hot-pressed α-SiC with aluminium additive and concluded that the addition of aluminium results in the presence of a second phase in the grain boundaries, which causes the appearance of an intergranular fracture pattern at high temperature.

Since the material used in the present work is β-SiC and it contains aluminium not as an additive but in the starting powder, the microstructure, particularly of the grain boundary, might be different (at least in parts) from that of the α-SiC used by Moussa *et al.* Accordingly, observation of the microstructure by TEM is needed, but since it seems that in the present S-2 material also aluminium doping enhances grain boundary deformation to produce intergranular fracture (Fig. 12), the mechanism of viscous sliding of grain boundaries through the second phase which Moussa *et al.* reported for α-SiC–Al seems to be applicable to the present S-2 material.

If such a damage mechanism is valid, it seems reasonable that the cyclic loading effect, which has to be essentially controlled by the plastic deformation due to dislocation movement, is not observed in S-2 material. In S-1 material which does not contain aluminium also, an insignificant effect of cyclic loading was observed in the present experimental conditions. Therefore, it is concluded that at elevated temperature (1500° C) in SiC materials there is no indication of the deformation which is related to dislocation motion.

4. Conclusions

Cyclic and static fatigue behaviours were investigated using sintered β-SiC materials having indented precracks, and attention was especially focused on the temperature dependence and the effect of aluminium doping. The results obtained are as follows.

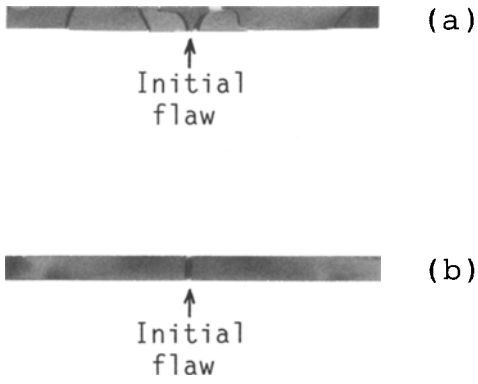

Figure 17 Specimens fractured in argon gas at 1500° C (indentation load 9.8 N): (a) S-1, (b) S-2.

1. No effects of cyclic loading were observed in the crack growth behaviour of two types of both materials with aluminium (S-1) and without aluminium (S-2) tested over the whole temperature range of room temperature to 1500° C, suggesting that cyclic fatigue might be insignificant in SiC.
2. However, there exists a static fatigue in such materials, the causes of which are interestingly different, depending upon the temperature and the aluminium doping.
3. The static fatigue observed at room temperature is environmentally assisted cracking.
4. At intermediate temperature in argon gas significant static fatigue was not observed, but slight damage (crack growth) was seen in S-2 though the reason for this is unclear.
5. The static fatigue at higher temperature (1500° C) seems to be controlled by the creep properties. In S-2 containing aluminium, intensive plastic deformation (assumed to occur mainly in grain boundaries) and intergranular cracking with crack tip blunting were observed, whereas in S-1 a higher resistance to creep deformation and healing of the initial flaws were seen at the same temperature of testing. It is concluded, therefore, that aluminium doping of the SiC material makes its strength decrease for the case where the material is loaded to failure in a short time (for example at high stresses), but makes the resistance to cracking rather increase for the case where it is statically loaded at lower stresses for a relatively long time.

Acknowledgement

This study was supported by the "Special Coordination Funds for Promoting Science and Technology" of the Science and Technology Agency of the Japanese Government.

References

1. R. KOSSOWSKY, *J. Amer. Ceram. Soc.* **56** (1973) 531.
2. *Idem*, in "Ceramics for High Performance Applications", edited by J. J. Burke, A. F. Gorum and R. N. Katz (Brook Hill, 1974) p. 347.
3. M. KAWAI, H. FUJITA, Y. KANKI, H. ABE and J. NAKAYAMA, in "Proceedings of International Symposium on Ceramic Components for Engines", 1983, p. 269.

4. S. ITO, Y. YAMAUCHI, M. ITO and S. SAKAI, *Proc. Jpn Congr. Mater. Res.* **26** (1983) 270.
5. T. KAWAKUBO and K. KOMEYA, *J. Soc. Mater. Sci. Jpn* **34** (1985) 1460.
6. S. HORIBE, *J. Mater. Sci. Lett.*
7. S. C. SANDAY, *Int. Congr. Combust. Engines* **12** (1977) 2543.
8. A. G. EVANS and F. F. LANGE, *J. Mater. Sci.* **10** (1975) 1659.
9. D. B. MARSHALL and B. R. LAWN, *J. Amer. Ceram. Soc.* **63** (1980) 532.
10. J. J. PETROVIC and L. A. JACOBSON, *ibid.* **59** (1976) 34.
11. J. J. PETROVIC, R. A. DIRKS, L. A. JACOBSON and M. G. MENDIRATTA, *ibid.* **59** (1976) 177.
12. H. TANAKA, Y. INOMATA and H. KAWABATA, *J. Ceram. Soc. Jpn* **88** (1980) 570.
13. G. GRATHWOHL, T. H. REETS and F. THÜMMLER, *Sci. Ceram.* **11** (1981) 425.
14. R. MOUSSA, F. OSTERSTOCK and J.-L. CHERMANT, in "Fracture Mechanics of Ceramics 6", edited by R. C. Bradt, A. G. Evans, D. P. H. Hasselman and F. F. Lange (Plenum, New York, 1983) p. 555.
15. J. L. CHERMANT and F. OSTERSTOCK, *Mater. Sci. Engng* **71** (1985) 147.

Received 22 September 1987
and accepted 26 January 1988